

Cross section data node:

Ion and atom collisions with neutrals

June 2019

Prepared by: H.N. Williamson and R.E. Johnson

University of Virginia

Charlottesville, VA 22904

Configuration Management Plan

This document was supported by the PDART (Planetary Data Archiving Restoration and Tools) program. Proposed changes and questions or comments regarding this document should be submitted to either R.E. Johnson (rej@virginia.edu) or H.N. Williamson (hwn9ew@virginia.edu). If changes are suggested they should be accompanied by supporting material.

Cross Sections – PDS Atmospheres Node

TABLE OF CONTENTS

- 1. INTRODUCTION:**
 - 1.1 Purpose and Scope**
 - 1.2 Contents**
 - 1.3 Data Bases**
 - 1.4 Cross Sections**
 - 1.5 Definitions and Coordinate Systems**
 - 1.6 Angular Scattering**
 - 1.7 Introduction References**
- 2. Management**
- 3. Data and References**

Cross Sections – PDS Atmospheres Node

Acronyms & Definitions

σ (total cross section in m^2)

σ_d (diffusion/ momentum transfer cross section in m^2)

σ_{CT} (cross section for charge transfer in m^2 : $A^+ + B \rightarrow A + B^+$)

$\sigma_{AB \rightarrow CD}$ (reaction cross section in m^2 : $A + B \rightarrow C + D$)

Ω (solid angle in steradians)

$d\sigma/\Omega$ (cross section per unit solid angle)

χ (center of mass scattering angle)

θ (laboratory scattering angle)

ϕ (azimuthal scattering angle)

\mathbf{v} (relative velocity between colliding particles)

v (size of \mathbf{v})

\mathbf{v}_i (velocity of one of the colliding particles)

b (impact parameter: the distance between colliding particles perpendicular to \mathbf{v})

Σ (a summation)

CM (center of mass system)

n local number density (atoms or molecules per unit volume)

m mass of an atomic or molecular species

ρ mass density (mn for a single species atmosphere)

g gravitational acceleration

T ambient temperature in an equilibrium region

k Boltzmann constant

H scale height for a species of mass $= kT/mg$

mfp mean free path of a collision $(c \sigma_d n)^{-1}$ where c is a number near to unity depending on the dependence of σ_d on the relative speed of the colliding particles.

exobase (the altitude in a gravitationally bound atmosphere from which an energized atom or molecule can escape with a high probability: called nominal exobase as it depends on the species escaping; often $H = mfp$ for a collision on an escaping species with the ambient species)

exosphere (the region of the atmosphere above the nominal exobase)

Cross Sections – PDS Atmospheres Node

1. INTRODUCTION

1.1 Purpose and Scope

This document describes cross data of interest to modeling and simulations of the behavior of the exobase region of an atmosphere gravitationally bound to a planet or a planetary satellite in order to describe thermal or plasma induced escape or to be used to describe scattering processes occurring in a planetary torus consisting of neutrals and ions. The cross section data is made available for use in various Monte Carlo modeling of these regimes, either ballistic modeling or molecular kinetic simulations, essentially numerical solutions to the Boltzmann equations. The available data will be archived in the Planetary Atmospheres Discipline Node (ATM) of the Planetary Data System (PDS) that includes references to sources both of calculations and laboratory measurements of various cross sections.

1.2 Contents Database

This archive contains certain cross section data that has been measured or calculated for use in modeling planetary atmospheres listed under Archived Data with references given. The data presented here is not complete but can be supplemented by cross section models that can be estimated from on line software and by data stored on other web sites. Most of the data is for total reaction cross sections and not differential cross sections, results that are needed for determining the scattering angles for a given process. However, angular scattering is discussed below, as well as some methods for modeling or extrapolating cross sections and follows the methods discussed in Johnson (1990)

The data relevant to upper atmosphere on various bodies varies considerably depending on its content. For the giant planets this is typically H, H₂ and He interacting with each other, with their ions, and often with trace species. For the terrestrial planets and related small bodies, nitrogen, oxygen and carbon species typically dominate. These molecules can be strongly gravitationally bound or even rapidly escaping as in a comet. Therefore, many useful websites have been constructed for relevant planetary objects containing for cross section data that supplements what is in this archive.

1.3 Databases

List of Astrochemistry Databases:

[astrochmehttp://www.astrochemistry.eu/ac/astrochem_databases.html](http://www.astrochemistry.eu/ac/astrochem_databases.html)

List of Databases for Atomic and Plasma Physics

<http://plasma-gate.weizmann.ac.il/directories/databases/>

IPPJ-publications of data:

<http://dpc.nifs.ac.jp/IPPJ-AM/IPPJ-AM-list.html>

NIFS DATABASE

<https://dbshino.nifs.ac.jp/>

The Virtual Atomic and Molecular Data Centre (VAMDC)

<http://www.vamdc.eu>

Leiden Atomic and Molecular Database

<https://home.strw.leidenuniv.nl/~moldata/>

Basic Science Data Center

<http://www.camdb.ac.cn/e/>

Cloudy: Photoionization Simulations

<https://www.nublado.org/wiki/StoutData>

1.4 Cross Sections

The concept of a cross section can roughly be described by imagining and experiment in which a flux of particles A, $\Phi_A(0)$, moves in a direction \mathbf{z} through a background of randomly distributed atoms or molecules B. That flux is disrupted by collisions so that after a distance z , the flux of particles having *not* collided depends roughly exponentially on the distance traveled by particles A and is written as $\Phi_A(z) = \Phi_A(0) \exp(-z/\lambda_{AB})$. The extracted parameter from such a measurement, λ_{AB} , is called the mean free path for a collision of A with B. As the likelihood of a collision must depend inversely on the number density of B, n_B , one writes, $\lambda_{AB} = (\sigma_{AB} n_B)^{-1}$. The parameter extracted from such an experiment, σ_{AB} , has units of area and is called the cross section, a measure of the likelihood of a collision of A with B. More information on the collisions can be obtained if the scattering angles are also measured. For a flux of incident particles transiting a gas, the probability of a particle scattered into a unit solid angle, $d\Omega_A = \sin\theta_A d\theta_A d\phi_A$, is related to the incident flux by the differential cross section $[d\sigma_{AB}/d\Omega_A]$, with θ_A and ϕ_A , the angles into which A is scattered shown schematically in Fig 1 below. This cross section, of course, depends in some detail on the forces and speeds of the colliding particles, with σ_{AB} equal to the integral of the differential cross section over all solid angles: $\sigma_{AB} = \int [d\sigma_{AB}/d\Omega_A] d\Omega_A$. The azimuthally averaged differential cross $[d\sigma_{AB}/d\Omega_A]$ is often written for simplicity as $\sigma_{AB}(\theta_A)$. The corresponding section for the azimuthally averaged scattered target particle, $[d\sigma_{AB}/d\Omega_B] = \sigma_{AB}(\theta_B)$, can also be measured or, for elastic scattering, determined from the result for A (Johnson 1990; Johnson and Bowman 2003).

1.5 Definitions and Coordinate Systems

Although the data presented here are primarily integrated cross sections, in applying these in Monte Carlo simulations the angular dependences are needed. These can be available in a number of the references given. Two coordinate systems are typically used for describing the exiting velocities of the particles after a collision. These are the so-called laboratory system in which it is assumed that a moving atom, molecule or ion interacts with a stationary target atom or molecule as in Figure 1, and the center of mass coordinate system in Figure 2, discussed below. Data in either system can be modified by a translation if the colliding particles are moving at different speeds. In the typical definition of the laboratory system, the two colliding particles are shown as being spherically symmetric. When that is not the case, as when a target or incident particle is a molecule, then the results of models and of laboratory data are often spherically averaged values of more detailed cross section measurements or models. When spherical averaging is not carried out a much more detailed coordinate system is needed for calculating cross sections for an incident molecular ion or neutral colliding with a molecule. Then, when relating to typical laboratory data, averaging over incident and exiting orientations is carried out.

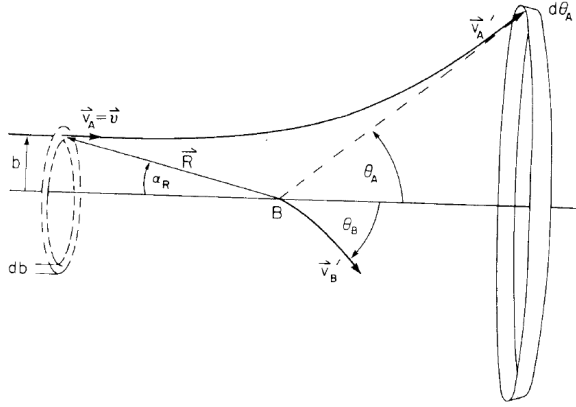


Fig. 1 Laboratory System: Scattering of particle A with an initial velocity \mathbf{v}_A by particle B with $\mathbf{v}_B = 0$. \mathbf{R} is the radial distance from the origin of the coordinate system, which is the initial position of B; b is the impact parameter ($b = |\mathbf{R} \times \mathbf{v}_A / v_A|$ the perpendicular distance from the direction of the incident particle; α_R is the orientation angle; θ_A and θ_B are the scattering angles of A and B; \mathbf{v}_A' and \mathbf{v}_B' are the velocities of the scattered particles; $2\pi \sin\theta_A d\theta_A$ is the solid angle of acceptance for the scatter particle A.

If the forces acting in Fig. 1 depend only on the radial distance between A and B, or if there are random orientation, then on average particles passing through the ring of area $2\pi b db$ will be scattered into the angular ring $2\pi \sin\theta_A d\theta_A$. Therefore, knowing the how θ_A depends on b , one can in principal calculate $b(\theta_A)$, or $\theta_A(b)$, the deflection function. The differential cross section is then calculated as $\sigma_{AB}(\theta_A) = |b db / \sin\theta_A d\theta_A|$.

In Fig. 2 we show the, so-called, center of mass (CM) coordinate system with the same spherical assumptions as in Fig. 1. Cross section models are often calculated in this system of coordinates, as discussed below. That is, knowing the forces between the particles one can determine how χ depends on b . That is, one can in principal calculate $\chi(b)$, the CM deflection function. The differential cross section is then calculated as $\sigma_{AB}(\chi) = |b db / \sin\chi d\chi|$.

The symbol used here for the azimuthally averaged differential cross section is $\sigma_{AB}(\chi)$, so that $\sigma_{AB} = 2\pi \int \sigma_{AB}(\chi) \sin\chi d\chi$. Also shown in Fig. 2 is the translation to the laboratory coordinate system with the conversion of quantities between these systems given in Table 1.

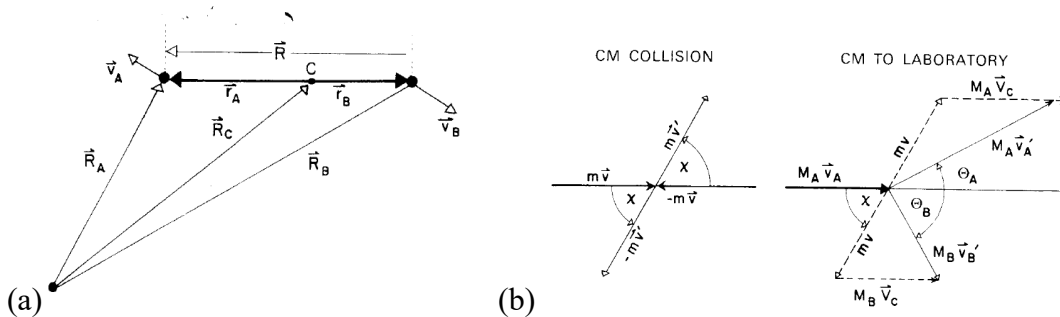


Fig2. (a) Center of mass (CM) system: \mathbf{R}_A and \mathbf{R}_B the location of A and B; \mathbf{R} the distance between A and B. C the location of the center on mass: $\mathbf{R}_C = (M_A \mathbf{R}_A + M_B \mathbf{R}_B) / (M_A + M_B)$; \mathbf{r}_A and \mathbf{r}_B , location of A and B in CM system; relative velocity $\mathbf{v} = \mathbf{v}_A - \mathbf{v}_B$, velocity of the CM: $d\mathbf{R}_C/dt = \mathbf{V}_C = (M_A \mathbf{v}_A + M_B \mathbf{v}_B) / (M_A + M_B)$. (b) Scattering in CM converted to laboratory system in Fig. 1: χ , scattering angle in the CM; $m = M_A M_B / (M_A + M_B)$ the reduced mass in CM system.

Table 1. Conversion of CM to Lab Quantities*

Velocity of CM	$\vec{V}_c = (M_A \vec{v}_A + M_B \vec{v}_B)/(M_A + M_B) \equiv \vec{R}_c$	
Relative velocity in CM	$\vec{v} = (\vec{v}_A - \vec{v}_B) \equiv \vec{R}$	
Total laboratory quantities	CM quantities	
$M = M_A + M_B$	$m = M_A M_B / (M_A + M_B)$: mass
$E_A + E_B = M V_c^2 / 2 + E$	$E = m v^2 / 2$: energy
$M_A \vec{v}_A + M_B \vec{v}_B = M \vec{V}_c$	$\vec{P} = 0$: momentum
$\vec{L}_A + \vec{L}_B = M \vec{R}_c \times \vec{V}_c + \vec{L}$	$\vec{L} = m \vec{R} \times \vec{v}$: angular momentum
Transformations (for v_B initially zero and elastic collisions)		
$\theta_B = (\pi - \chi)/2$		
$\tan \theta_A = \mu \sin \chi / (1 + \mu \cos \chi); \mu = M_B / M_A$		
$T = \gamma E_A \sin^2 (\chi/2); \gamma = 4 M_B M_A / (M_A + M_B)^2$		
$(d\sigma/d\Omega)_A = \sigma(\chi)$	$\left \frac{d\cos\chi}{d\cos\theta_A} \right = \sigma(\chi) \frac{(\mu^2 + 2\mu\cos\chi + 1)^{3/2}}{\mu^2 \mu + \cos\chi }$	
$(d\sigma/d\Omega)_B = \sigma(\chi)$	$\left \frac{d\cos\chi}{d\cos\theta_B} \right = \sigma(\chi) 4 \sin(\chi/2) $	
$\frac{d\sigma}{dT} = \frac{4\pi}{\gamma E_A} \sigma(\chi)$		

* $d\Omega_A = \sin\theta_A d\theta_A d\phi_A \rightarrow d\cos\theta_A d\phi_A$ and $d\Omega_B = \sin\theta_B d\theta_B d\phi_B \rightarrow d\cos\theta_B d\phi_B$ are the differential solid scattering angles in laboratory system in Fig. 1, though azimuthal angles for each particle, ϕ_A and ϕ_B , are not indicated.

In addition, impact parameter models for cross sections are often used since the ‘closeness’ of the collision between particles is determined in part by the impact parameter, b in Fig. 1, and it in turn can determine the outcome. Therefore, the outcome from a reactive collision, $A + B \rightarrow C + D$, is often written as:

$$\sigma_{A+B \rightarrow C+D} = \int_0^\infty P_{A+B \rightarrow C+D} 2\pi b db$$

where $P_{A+B \rightarrow C+D}$ is the transition or reaction probability. It depends on b , the closeness of the collision, as well as the relative speed, v , of the colliding species which determines the time spent interacting. Chemists and physicists often have simple models for estimating this probability as the reactions often occur when the collision is sufficient close and/or sufficiently energetic to overcome a barrier. Or, if particles are imagined to have radii r_A and r_B , one often approximate a total collision cross section, $\sigma_{AB} \sim \sigma_c$, assuming that $P_c = 1$ for $b < (r_A + r_B)$ and zero otherwise, so $\sigma_c = \pi(r_A + r_B)^2$. This procedure is referred to as the hard sphere collision cross section, still used, but often not very accurate. For hard spheres, the scattering in the CM system is isotropic making it easy to use in computational models.

Often one only requires the spatial distribution of energy deposition of incident plasma ions or neutrals in a gas: e.g., the energy deposited by solar wind or magnetospheric ions in an atmosphere. The SRIM website (www.srim.org) developed by Zeigler uses universal cross sections based on scaling to a large set of experimental data. This web site calculates the cascade of collisions that is set in motion by an incident ion or neutral in a material. One runs simulations that not only give the spatial distribution of the energy deposited in excitations and in momentum transfer, but also the spatial distribution of the excited recoils. This was developed for solids but has been applied as a rough approximation for a flux of particles entering an atmosphere, as the density can be chosen. Since the production of recoils can lead to ejection of material (a process often called sputtering) sputter yields are also given using this software. Based on the discussion in Johnson (1990) such yields can be adapted and used to describe ejection of atoms and molecules from an atmosphere, often referred to as atmospheric sputtering.

1.6 Angular Scattering

Angular scattering cross section calculations are typically carried out in the CM system. Such calculations can then be translated, as needed, to the laboratory system or, in a simulation, to the cases in which both particles are moving, as discussed above. Using an impact parameter concept the CM scattering angle χ for an azimuthally averaged interaction can be calculated classically, semi-classically or by fully quantum mechanical methods from an interaction potential function, $V(R)$. For the collision of between atoms and molecules, the relationship between these methods has been examined for a number of systems: (e.g., O + O Tully and Johnson 2001; N + N₂ Tully and Johnson 2002). For low energy molecular collisions, classical scattering calculations can usefully give the angular scattering results.

The various scattering approximations can be used to determine the deflections as a function of b : $\chi(b)$ discussed above. Using the calculated $\chi(b)$, the angular scattering cross section is determined from $\sigma_{AB}(\chi) = \left| b \, db / \sin \chi \, d\chi \right|$. However, there is often more than one interaction potential, as is the case even for the important interaction O + O for which there are 18 ground state interactions. The resulting $\sigma_{AB}(\chi)$ calculated using each the interaction potential for each state can be averaged, weighted by the statistical importance of each state (Tully and Johnson 2001).

The analytic formula for the scattering function, $\chi(b)$, calculated classically for spherical potentials is given in many texts, but for complicated interactions can be calculated numerically. The often used estimate for fast incident particles in which the cross section is dominated by small deflection angles is the impulse approximation: $\chi(b) \sim - \{d[\int V(R) \, dz] / db\} / (2E)$. Assuming a nearly straight-line trajectory for a small deflection one integrates the force between the particles from $-\infty$ to $+\infty$ using the particular interaction potential between A and B, $V(R)$. In this approximation, $R^2 = b^2 + z^2$ and E is the energy in the CM in Table 1.

Because the cross section size is indeed often determined by small angle scattering, the impulse approximation has proven to be useful. Based on the expression above, the quantity $\tau = (\chi(b) E)$ is seen to only depend on the nature of the interaction potential. In the laboratory system, τ can be written as $\tau \sim (\theta_A E_A)$. Therefore, one can usefully scale the cross section data using what has been called a (ρ, τ) plot, with $\rho = \chi \sin \chi$ $\sigma_{AB}(\chi) \sim \theta_A \sin \theta_A \sigma(\theta_A)$. In the impulse approximation this plot is independent of the

incident energy, so that measurements at a number of energies can be roughly displayed together. Therefore, a set of measured differential cross section data can be used to extend the range of its applicability of laboratory data and also then used to estimate angular scattering data for similar systems. From such a plot one can also extract or test an estimate of the interaction potential, $V(R)$, which can subsequently be used to construct relevant molecular scattering cross sections. The potentials extracted in this manner from laboratory data have also been used to determine molecular dissociation cross sections for atmospherically relevant molecules (Johnson and Liu 1998; Johnson et al. 2002). This procedure was also recently used to extend calculations of cross section data to a variety of collision partners relevant to the study of the upper atmosphere on Mars (Lewkow and Kharchenko 2014).

1.7 Introduction References

Johnson, R.E., Introduction to Atomic and Molecular Collisions, Plenum NY&London. (1982) (download chapters: <http://people.virginia.edu/~rej/book.html>)

Johnson, R.E., Energetic Charged-Particle Interactions with Atmospheres and Surfaces Springer-Verlag, Berlin Heidelberg New York (1990) (download chapters: <http://people.virginia.edu/~rej/book.html>)

Johnson, R.E. and M. Liu, Sputtering of the atmosphere of Mars 1. Collisional dissociation of CO_2 , J. Geophys. Res. 103, 3639-3647 (1998)

Johnson, R.E., M. Liu, and C. Tully, Collisional Dissociations Cross Sections for $\text{O}^+ \text{O}_2$, CO and N_2 , O_2+O_2 , $\text{N}+\text{N}_2$, N_2+N_2 , Planetary and Space Science 50, 123-128 (2002)

Johnson, R.E. and J.M. Bowman. Atomic and Molecular Collisions in Encyclopedia of Physical Science and Technology (3rd edition) edited by R. A. Meyers (Academic Press, New York, 2003) <https://doi.org/10.1016/B0-12-227410-5/00040-5> <https://doi.org/10.1016/B0-12-227410-5/00040-5> Vol. 1 pp, 721-744 (2003)

Lewkow, N.R. & V. Kharchenko, Precipitation of energetic neutral atoms and induced non-thermal escape fluxes from the Martian atmosphere. Astrophysical Journal 790(2) (2014). doi:10.1088/0004-637X/790/2/98. URL <http://stacks.iop.org/0004-637X/790/i=2/a=98?key=crossref.e1d1418269b4a590ea9503c78aa33442>

Tully, C. and R.E. Johnson, Low energy collisions between ground-state oxygen atoms. Planetary and Space Science 49, 533–537 (2001).

Tully, C. and R.E. Johnson, Semiclassical calculation of collisional dissociation cross sections for $\text{N} + \text{N}_2$. J. Chem. Phys. 117, 6556-6561 (2002). Erratum 119, 10452-10453 (2003)

2. Management

3. List of Tables of Data Products

data_derived_co2

File Name	Process	Citation
co2andco2_candunknown	$\text{CO}_2 + \text{CO}_2 \Rightarrow \text{C} + ?$	Johnson and Liu (1998)
co2andco2_coandunknown	$\text{CO}_2 + \text{CO}_2 \Rightarrow \text{CO} + ?$	Johnson and Liu (1998)
coandco2_candoandunknown	$\text{CO} + \text{CO}_2 \Rightarrow \text{C} + \text{O} + ?$	Johnson and Liu (1998)
coandco2_coandcandunknown	$\text{CO} + \text{CO}_2 \Rightarrow \text{CO} + \text{C} + ?$	Johnson and Liu (1998)
coandco2_coandunknown	$\text{CO} + \text{CO}_2 \Rightarrow \text{CO} + ?$	Johnson and Liu (1998)

data_derived_helium

File Name	Process	Citation
heandar_unknown	$\text{He} + \text{Ar} \Rightarrow ?$	N. Lewkow (2018)
heandh_unknown	$\text{He} + \text{CO} \Rightarrow ?$	N. Lewkow (2018)
heandco_unknown	$\text{He} + \text{CO}_2 \Rightarrow ?$	N. Lewkow (2018)
heandco2_unknown	$\text{He} + \text{H} \Rightarrow ?$	N. Lewkow (2018)
heandh2_unknown	$\text{He} + \text{H}_2 \Rightarrow ?$	N. Lewkow (2018)
heandhe_unknown	$\text{He} + \text{He} \Rightarrow ?$	N. Lewkow (2018)
heandn2_unknown	$\text{He} + \text{N}_2 \Rightarrow ?$	N. Lewkow (2018)
heando_unknown	$\text{He} + \text{O} \Rightarrow ?$	N. Lewkow (2018)

data_derived_hydrogen

File Name	Process	Citation
handar_unknown	$\text{H} + \text{Ar} \Rightarrow ?$	N. Lewkow (2018)
handco_unknown	$\text{H} + \text{CO} \Rightarrow ?$	N. Lewkow (2018)
handco2_unknown	$\text{H} + \text{CO}_2 \Rightarrow ?$	N. Lewkow (2018)
handh_unknown	$\text{H} + \text{H} \Rightarrow ?$	N. Lewkow (2018)
handh2_unknown	$\text{H} + \text{H}_2 \Rightarrow ?$	N. Lewkow (2018)
handhe_unknown	$\text{H} + \text{He} \Rightarrow ?$	N. Lewkow (2018)
handn2_unknown	$\text{H} + \text{N}_2 \Rightarrow ?$	N. Lewkow (2018)
hando_unknown	$\text{H} + \text{O} \Rightarrow ?$	N. Lewkow (2018)
protonandh_2protonsande	$\text{H}^+ + \text{H} \Rightarrow \text{H}^+ + \text{H}^+ + \text{e}$	M. Shah (1998), M. Shah (1987)
protonandh_handproton	$\text{H}^+ + \text{H} \Rightarrow \text{H} + \text{H}^+$	J. Newman (1982), H. Tawara (1985), G. McClure (1966), P. Stier (1956)
protonandh_handunknown	$\text{H} + \text{H} \Rightarrow \text{H} + ?$	M. Rudd (1985)
protonandh2_2handproton	$\text{H}^+ + \text{H}_2 \Rightarrow \text{H} + \text{H} + \text{H}^+$	M. Shah (1989)
protonandh2_2protonsandhande	$\text{H}^+ + \text{H}_2 \Rightarrow \text{H}^+ + \text{H}^+ + \text{H} + \text{e}$	M. Shah (1989)

protonandh2_e	$H^+ + H_2 \Rightarrow e$	M. Rudd (1983)
protonandh2_hand2protonsande	$H^+ + H_2 \Rightarrow H + H^+ + H^+ + e$	M. Shah (1989)
protonandh2_handh2plus	$H^+ + H_2 \Rightarrow H + H_2^+$	G. McClure (1966), M. Shah (1989)
protonandh2_handunknown	$H^+ + H_2 \Rightarrow H + ?$	H. Tawara (1985), M. Rudd (1983)
protonandh2_protonandh2plusande	$H^+ + H_2 \Rightarrow H^+ + H_2^+ + e$	M. Shah (1989)
protonandh2o_h2oplusande	$H^+ + H_2O \Rightarrow H_2O^+ + e$	M. Rudd (1985)
protonandh2o_handh2oallplus	$H^+ + H_2O \Rightarrow H + (H_2O)^+$	F. Gobet (2001), J. Greenwood (2000), B. Lindsay (1997)
protonandh2o_handh2oplus	$H^+ + H_2O \Rightarrow H + H_2O^+$	F. Gobet (2001)
protonandh2o_handprotonandho	$H^+ + H_2O \Rightarrow H + H^+ + HO$	F. Gobet (2001)
protonandh2o_handunknown	$H^+ + H_2O \Rightarrow H + ?$	M. Rudd (1985)
protonandn_handnplus	$H^+ + N \Rightarrow H + N^+$	P. Stier (1956)
protonandn2_e	$H^+ + N_2 \Rightarrow e$	M. Rudd (1983)
protonandn2_hand2nplusande	$H^+ + N_2 \Rightarrow H + N^+ + N^+ + e$	H. Luna (2003)
protonandn2_handn2plus	$H^+ + N_2 \Rightarrow H + N_2^+$	B. Basu (1987), H. Luna (2003)
protonandn2_handndoubleplusandnande	$H^+ + N_2 \Rightarrow H + N^{++} + N + e$	H. Luna (2003)
protonandn2_handnplusandn	$H^+ + N_2 \Rightarrow H + N^+ + N$	H. Luna (2003)
protonandn2_handunknown	$H^+ + N_2 \Rightarrow H + ?$	M. Rees (1989), M. Rudd (1983)
protonandn2_protonand2nplusand2e	$H^+ + N_2 \Rightarrow H^+ + N^+ + N^+ + e + e$	H. Luna (2003)
protonandn2_protonandn2plusande	$H^+ + N_2 \Rightarrow H^+ + N_2^+ + e$	B. Basu (1987), H. Luna (2003)
protonandn2_protonandndoubleplusandnand2e	$H^+ + N_2 \Rightarrow H^+ + N^{++} + N + e + e$	H. Luna (2003), M. Shah (2008)
protonando_handodoubleplusande	$H^+ + O \Rightarrow H + O^{++} + e$	W. Thompson (1996)
protonando_handoplus	$H^+ + O \Rightarrow H + O^+$	W. Thompson (1996), B. Basu (1987), P. Stier (1956)
protonando_protonandoplusande	$H^+ + O \Rightarrow H^+ + O^+ + e$	W. Thompson (1996), B. Basu (1987)

protonando2_e	$H^+ + O_2 \Rightarrow e$	M. Rudd (1983)
protonando2_hand2oplusande	$H^+ + O_2 \Rightarrow H + O^+ + O^+ + e$	H. Luna (2004)
protonando2_hando2plus	$H^+ + O_2 \Rightarrow H + O_2^+$	B. Basu (1987), H. Luna (2004)
protonando2_handodoubleplusando	$H^+ + O_2 \Rightarrow H + O^{++} + O + e$	H. Luna (2004)
protonando2_handoplusando	$H^+ + O_2 \Rightarrow H + O^+ + O$	H. Luna (2004)
protonando2_handunknown	$H^+ + O_2 \Rightarrow H + ?$	M. Rudd (1983), M. Rees (1989)
protonando2_protonando2plusande	$H^+ + O_2 \Rightarrow H^+ + O_2^+ + e$	B. Basu (1987), H. Luna (2004)
protonando2_protonandodoubleplusandoand2e	$H^+ + O_2 \Rightarrow H^+ + O^{++} + O + e + e$	H. Luna (2004)
protonando2_protonandoplusando	$H^+ + O_2 \Rightarrow H^+ + O^+ + O + e$	H. Luna (2004)

data derived nitrogen

File Name	Process	Citation
n2andn2_4n	$N_2 + N_2 \Rightarrow N + N + N + N$	R. Johnson (2002)
n2plusandh2o_n2andh2oplus	$N_2^+ + H_2O \Rightarrow N_2 + H_2O +$	R. Dressler (1993)
n2plusandh2o_n2hplusandoh	$N_2^+ + H_2O \Rightarrow N_2H^+ + OH$	R. Dressler (1993)
n2plusando_unknown	$N_2^+ + O \Rightarrow ?$	R. Stebbings (1963)
nandn2_nandnandn	$N + N_2 \Rightarrow N + N + N$	R. Johnson (2002)
nandn2_unknown	$N + N_2 \Rightarrow ?$	C. Tully (2002)
ndoubleplusandh_nplusandunknown	$N^{++} + H \Rightarrow N^+ + ?$	H. Tawara (1985)
nplusandh_nandproton	$N^+ + H \Rightarrow N + H^+$	H. Tawara (1985), R. Phaneuf (1978)
nplusandh2_nandh2plus	$N^+ + H_2 \Rightarrow N + H_2^+$	R. Phaneuf (1978)
nplusandh2_nandunknown	$N^+ + H_2 \Rightarrow N + ?$	H. Tawara (1985), J. Hoffman (1982)
nplusandh2o_nandh2oplus	$N^+ + H_2O \Rightarrow N + H_2O^+$	R. Dressler (1994)
nplusandh2o_noplusandh2	$N^+ + H_2O \Rightarrow NO^+ + H_2$	R. Dressler (1994)
nplusandn2_2nandndoubleplusande	$N^+ + N_2 \Rightarrow N + N + N^{++} + e$	H. Luna (2003)
nplusandn2_2nandnplus	$N^+ + N_2 \Rightarrow N + N + N^+$	H. Luna (2003)

nplusandn2_3nplusand2e	$N^+ + N_2 \Rightarrow N^+ + N^+ + N^+ + e + e$	H. Luna (2003)
nplusandn2_nand2nplusande	$N^+ + N_2 \Rightarrow N + N^+ + N^+ + e$	H. Luna (2003)
nplusandn2_nandn2plus	$N^+ + N_2 \Rightarrow N + N_2^+$	W. Freysinger (1994), H. Luna (2003)
nplusandn2_nandunknown	$N^+ + N_2 \Rightarrow N + ?$	A. Phelps (1991), J. Hoffman (1982)
nplusandn2_nplusandndoubleplusandnand2e	$N^+ + N_2 \Rightarrow N^+ + N^{++} + N + e + e$	H. Luna (2003)
nplusandn2_unknown	$N^+ + N_2 \Rightarrow ?$	R. Stebbings (1963)
nplusando_nandoplus	$N^+ + O \Rightarrow N + O^+$	R. Stebbings (1963), H. Lo (1971)

data_derived_oxygen

File Name	Process	Citation
o2ando2_4o	$O_2 + O_2 \Rightarrow O + O + O + O$	R. Johnson (2002)
o2plusando_unknown	$O_2^+ + O \Rightarrow ?$	R. Stebbings (1963b)
o2plusando2_unknown	$O_2^+ + O_2 \Rightarrow ?$	R. Stebbings (1963a)
o3pando3p_unknown	$O(^3P) + O(^3P) \Rightarrow ?$	C. Tully (2001)
oandco_oandcando	$O + CO \Rightarrow O + C + O$	R. Johnson (2002)
oandco2_2oandco	$O + CO_2 \Rightarrow O + O + CO$	Johnson and Liu (1998)
oandco2_3oandc	$O + CO_2 \Rightarrow O + O + O + C$	Johnson and Liu (1998)
oandn2_oandnandn	$O + N_2 \Rightarrow O + N + N$	R. Johnson (2002)
oando2_oandoando	$O + O_2 \Rightarrow O + O + O$	R. Johnson (2002)
odoubleplusandh_oplusandproton	$O^{++} + H \Rightarrow O^+ + H^+$	R. Phaneuf (1978)
odoubleplusandh_oplusandunknown	$O^{++} + H \Rightarrow O^+ + ?$	H. Tawara (1985)
odoubleplusandh2_oandunknown	$O^{++} + H_2 \Rightarrow O + ?$	H. Tawara (1985)
odoubleplusandh2_oplusanddh2plus	$O^{++} + H_2 \Rightarrow O^+ + H_2^+$	R. Phaneuf (1978)
odoubleplusandh2_oplusanddunknown	$O^{++} + H_2 \Rightarrow O^+ + ?$	H. Tawara (1985)
oplus2d2pandh2_oandunknown	$O^+(^2D, ^2P) + H_2 \Rightarrow O + ?$	Y. Xu (1990), D. Sieglaff (1999), R. Phaneuf (1978)
oplus2d2pando_oandoplus	$O^+(^2D, ^2P) + O \Rightarrow O + O^+$	B. Lindsay (2001)
oplus2dandh2_oandunknown	$O^+(^2D) + H_2 \Rightarrow O + ?$	T. Moran (1978)

oplus4sandh2_oandunkno wn	$O^+(^4S) + H_2 \Rightarrow O + ?$	G. Flesch (1991), Y. Xu (1990), A. Irvine (1991), D. Sieglaff (1999), W. Nutt (1979), J. Hoffman (1982), T. Moran (1978), R. Phaneuf (1978)
oplus4sandn2_noplusandn	$O^+(^4S) + N_2 \Rightarrow NO^+ + N$	G. Flesch (1990), X. Li (1997)
oplus4sandn2_nplusandnan do	$O^+(^4S) + N_2 \Rightarrow N^+ + N + O$	G. Flesch (1990), X. Li (1997), M. Shah (2008)
oplus4sandn2_oandn2plus	$O^+(^4S) + N_2 \Rightarrow O + N_2^+$	G. Flesch (1990), B. Lindsay (1998), X. Li (1997), M. Shah (2008)
oplus4sando_oandoplus	$O^+(^4S) + O \Rightarrow O + O^+$	B. Lindsay (2001)
oplusandh_oandproton	$O^+ + H \Rightarrow O + H^+$	H. Tawara (1985), R. Phaneuf (1987), T. Jorgensen (1965)
oplusandh_oplusandproton ande	$O^+ + H \Rightarrow O^+ + H^+ + e$	T. Jorgensen (1965)
oplusandh2_oandh2plus	$O^+ + H_2 \Rightarrow O + H_2^+$	R. Phaneuf (1978)
oplusandh2_oandunknown	$O^+ + H_2 \Rightarrow O + ?$	H. Tawara (1985)
oplusandh2o_oandh2oplus	$O^+ + H_2O \Rightarrow O + H_2O^+$	R. Dressler (1996)
oplusandh2o_ohplus	$O^+ + H_2O \Rightarrow OH^+$	D. Levandier (1996)
oplusandn2_oand2nplusan de	$O^+ + N_2 \Rightarrow O + N^+ + N^+ + e$	M. Shah (2008)
oplusandn2_oandndoublepl usandnande	$O^+ + N_2 \Rightarrow O + N^{++} + N + e$	M. Shah (2008)
oplusandn2_oplusand2nplu sand2e	$O^+ + N_2 \Rightarrow O^+ + N^+ + N^+ + e + e$	M. Shah (2008)
oplusandn2_oplusandn2plu sande	$O^+ + N_2 \Rightarrow O^+ + N_2^+ + e$	M. Shah (2008)
oplusandn2_oplusandndou bleplusandnand2e	$O^+ + N_2 \Rightarrow O^+ + N^{++} + N + e + e$	M. Shah (2008)
oplusando_2oplusande	$O^+ + O \Rightarrow O^+ + O^+ + e$	T. Jorgensen (1965)
oplusando_oandoplus	$O^+ + O \Rightarrow O + O^+$	T. Jorgensen (1965), H. Lo (1971), M. McGrath (1989)
oplusando2_2oandodouble plusande	$O^+ + O_2 \Rightarrow O + O + O^{++} + e$	H. Luna (2004)
oplusando2_2oandoplus	$O^+ + O_2 \Rightarrow O + O + O^+$	H. Luna (2004)
oplusando2_3oplusand2e	$O^+ + O_2 \Rightarrow O^+ + O^+ + O^+ + e + e$	H. Luna (2004)
oplusando2_oand2oplusan de	$O^+ + O_2 \Rightarrow O + O^+ + O^+ + e$	H. Luna (2004)
oplusando2_oando2plus	$O^+ + O_2 \Rightarrow O + O_2^+$	H. Luna (2004)

oplusando2_oplusando2plusande	$O^+ + O_2 \Rightarrow O^+ + O_2^+ + e$	H. Luna (2004)
oplusando2_oplusandodoubleplusandoand2e	$O^+ + O_2 \Rightarrow O^+ + O^{++} + O + e + e$	H. Luna (2004)
oplusando2_unknown	$O^+ + O_2 \Rightarrow ?$	R. Stebbings (1963)
oplusands_oandsplus	$O^+ + S \Rightarrow O + S^+$	M. McGrath (1989)

data derived sodium

File Name	Process	Citation
naande_napland2e	$Na + e \Rightarrow Na^+ + e + e$	Johnston (1995), Zapes (1969)
naplandk_naandkplus	$Na^+ + K \Rightarrow Na + K^+$	L. Pivovar (1969), M. McGrath (1989)
naplandna_naandnapland	$Na^+ + Na \Rightarrow Na + Na^+$	M. McGrath (1989)
naplands_naandsplus	$Na^+ + S \Rightarrow Na + S^+$	M. McGrath (1989)

data derived sulfur

File Name	Process	Citation
sdoubleplusando_splandoplus	$S^{++} + O \Rightarrow S^+ + O^+$	M. McGrath (1989)
sdoubleplusandodoubleplus_stripleplusandoplus	$S^{++} + O^{++} \Rightarrow S^{+++} + O^+$	M. McGrath (1989)
splando_sandoplus	$S^+ + O \Rightarrow S + O^+$	M. McGrath (1989)
splands_sandsplus	$S^+ + S \Rightarrow S + S^+$	M. McGrath (1989)
splandsdoubleplus_sdoupleplusandsplus	$S^+ + S^{++} \Rightarrow S^{++} + S^+$	M. McGrath (1989)

data derived water

File Name	Process	Citation
h2oande_h2oplusand2e	$H_2O + e \Rightarrow H_2O^+ + e + e$	O. Orient (1987), M. Rao (1995)
h2oande_h2plusandoand2e	$H_2O + e \Rightarrow H_2^+ + O + e + e$	H. Straub (1998)
h2oande_odoubleplusandh2and2e	$H_2O + e \Rightarrow O^{++} + H_2 + e + e$	H. Straub (1998)
h2oande_ohplusandhand2e	$H_2O + e \Rightarrow OH^+ + H + e + e$	O. Orient (1987)
h2oande_ohplusandprotonand3e	$H_2O + e \Rightarrow OH^+ + H^+ + e + e + e$	M. Rao (1995)
h2oande_oplusandh2and2e	$H_2O + e \Rightarrow O^+ + H_2 + e + e$	O. Orient (1987), M. Rao (1995), H. Straub (1998)
h2oande_protonandohand2e	$H_2O + e \Rightarrow H^+ + OH + e + e$	O. Orient (1987), M. Rao (1995), H. Straub (1998)

h2oplusandh2o_h2oandh2oplus	$\text{H}_2\text{O} + \text{H}_2\text{O} \Rightarrow \text{H}_2\text{O} + \text{H}_2\text{O}^+$	C. Lishawa (1990)
h2oplusandh2o_h3oplusandoh	$\text{H}_2\text{O}^+ + \text{H}_2\text{O} \Rightarrow \text{H}_3\text{O}^+ + \text{OH}$	C. Lishawa (1990)

List of Citations Used

Basu, B., Jasperse, J.R., Robinson, R.M., Vondrak, R.R., Evans, D.S. (1987), Linear transport theory of auroral proton precipitation: A comparison with observations. *Journal of Geophysical Research* 92, 5920. 10.1029/JA092iA06p05920

Description: In this paper we present nearly coincident Chatanika radar electron density measurements and NOAA 6 particle data for a continuous (diffuse) auroral E layer with a peak electron density of $1\text{-}2 \times 10^5 \text{ cm}^{-3}$ produced entirely by proton precipitation.

Dressler, R.A., Bastian, M.J., Levandier, D.J., Murad, E. (1996), Empirical model of the state-to-state dynamics in near-resonant hyperthermal $\text{X}^+ + \text{H}_2\text{O}$ charge-transfer reactions. *International Journal of Mass Spectrometry and Ion Processes* 159, 245. 10.1016/S0168-1176(96)04454-0

Description: $\text{H}_2\text{O} + \text{A-X}$ luminescence studies involving $\text{X}^+ + \text{H}_2\text{O}$ ($\text{X} = \text{Ar}, \text{N}, \text{Kr}, \text{N}_2$) charge-transfer systems are consolidated into an empirical model for the charge-transfer product state distributions associated with hyperthermal collisions of ground-state reactants.

Dressler, Rainer and Murad, Edmond. (1994), Guided-ion beam measurements of $\text{N}^+ + \text{H}_2\text{O}$ charge-transfer and chemical reaction channels. *Chemical Physics - CHEM PHYS*. 100. 5656-5665. 10.1063/1.467275

Description: Guided-ion beam measurements of $\text{N}^+ + \text{H}_2\text{O}$ charge-transfer and chemically reactive channels are presented for collision energies ranging from 0.1 eV to 20 eV c.m.

Dressler, R.A., Salter, R.H., Murad, E. (1993), Guided-ion beam measurements of the $\text{X}^+ + \text{H}_2\text{O}$ (D_2O) ($\text{X} = \text{Ar}, \text{N}_2$) collision systems. *Journal of Chemical Physics* 99, 1159. 10.1063/1.465413

Description: Guided-ion beam cross section and product kinetic energy measurements of charge-transfer and atom-abstraction reactions of the $\text{Ar}^+ + \text{H}_2\text{O}(\text{D}_2\text{O})$ and $\text{N}_2^+ + \text{H}_2\text{O}(\text{D}_2\text{O})$ collision systems are presented for collision energies ranging between 0.2 and 20 eV c.m.

Flesch, G.D., Ng, C.Y. (1991), Absolute total cross sections for the charge transfer and dissociative charge transfer channels in the collisions of $\text{O}^+(^4\text{S}) + \text{H}_2$. *Journal of Chemical Physics* 94, 2372. 10.1063/1.459859

Description: Absolute total cross sections for the reactions, $\text{O}^+(^4\text{S}) + \text{H}_2$ to $\text{O} + \text{H}_2^+$ [reaction (1)] and $\text{O} + \text{H} + \text{H}^+$ [reaction (2)] have been measured in the center-of-mass collision energy ($E_{\text{c.m.}}$) range of 1.33-22.22 eV.

Freysinger, W. et al. (1994), Charge-transfer reaction of 14,15 $N^+(^3PJ) + N_2(1)$ from thermal to 100 eV Crossed-beam and scattering-cell guided-ion beam experiments, J. Chem. Phys. 101, 3688-3695. 10.1063/1.467553

Description: We have studied the charge-transfer reaction of $N^+(^3PJ)$ ions with N_2 from thermal to 40 and 100 eV in the center-of-mass frame with the Utah guided-ion beam mass spectrometer and the Trento crossed-beam guided-ion beam experiment.

Greenwood, J.B., Chutjian, A., Smith, S.J. (2000), Measurements of Absolute, Single Charge-Exchange Cross Sections of H^+ , He^+ and He_2^+ with H_2O and CO_2 . The Astrophysical Journal 529, 605. 10.1086/308254

Description: Absolute measurements have been made of single-electron charge-exchange cross sections of H^+ , He^+ and He_2^+ with H_2O and CO_2 in the energy range 0.3-7.5 keV amu^{-1} .

Gobet, F., et al. (2001), Total, Partial, and Electron-Capture Cross Sections for Ionization of Water Vapor by 20-150 keV Protons. Physical Review Letters 86, 3751. 10.1103/PhysRevLett.86.3751

Description: We present experimental results for proton ionization of water molecules based on a novel event by event analysis of the different ions produced (and lost).

Hoffman, J.M., Miller, G.H., and Lockwood, G.J. (1982), Charge transfer of ground-state C^+ , N^+ , and O^+ in N_2 and H_2 . Phys. Rev. A. 25. 10.1103/PhysRevA.25.1930

Description: The single-electron charge-transfer cross sections for ground-state C^+ , N^+ , and O^+ ions colliding with N_2 and H_2 are reported.

Irvine, A.D., Latimer, C.J. (1991), Charge transfer reactions of ground state O^+ ions with H_2 molecules. Journal of Physics B Atomic Molecular Physics 24, L145. 10.1088/0953-4075/24/5/007

Description: Cross sections for charge transfer between ground state (4S) O^+ ions in H_2 have been measured within the energy range 0.1-1.0 keV.

Johnson, R.E., Liu, M., Tully, C. (2002), Collisional dissociation cross sections for $O+O_2$, CO and N_2 , O_2+O_2 , $N+N_2$, and N_2+N_2 . Planetary and Space Science 50, 123. 10.1016/S0032-0633(01)00067-8

Description: Using laboratory data for the scattering of O by O_2 , CO and N_2 pair potentials are constructed for O, C and N atoms. These potentials are then used to calculate collisional dissociation and energy transfer cross sections for O on O_2 , CO and N_2 , O_2 on O_2 , N on N_2 , and N_2 on N_2 .

Johnson, R.E., Liu, M. (1998), Sputtering of the atmosphere of Mars 1. Collisional dissociation of CO_2 . Journal of Geophysical Research 103, 3639. 10.1029/97JE03265

Description: In this paper, we calculate dissociation cross sections for $O+CO_2$, $O+CO$, $CO+CO_2$, and CO_2+CO_2 collisions in the energy range 20 eV to 1 keV. Semiempirical interaction potentials are used from which cross sections are calculated via classical molecular dynamics.

Jorgensen, T., Kuyatt, C.E., Lang, W.W., Lorents, D.C., Sautter, C.A. (1965), Measurements on Charge-Changing Collisions Involving Negative Hydrogen, Helium, and Oxygen Ions. *Physical Review* 140, 1481. 10.1103/PhysRev.140.A1481
Description: Beams of H^+ , He^+ , and O^+ were sent through a gas cell where charge exchange took place. Ratios of various charge components were obtained for thick targets. Negative ion beams were sent through thin targets in a magnetic field and attenuation ratios were determined. Measurements were in the energy range from 10 to 400 keV.

Levandier, D.J., Dressler, R.A., Murad, E. (1996), A study of isotope effects in the reaction $\text{O}^+ + \text{H}_2\text{O}/\text{D}_2\text{O}$ to $\text{OH}^+/\text{OD}^+ + \text{OH}/\text{OD}$ using guided-ion beams. *Chemical Physics Letters* 251, 174. 10.1016/0009-2614(96)00069-3
Description: Guided-ion beam methods were used to measure the absolute cross sections for OH^+/OD^+ derived from O^+ and $\text{H}_2\text{O}/\text{D}_2\text{O}$ collisions over the range of 0.25-20 eV relative energy.

Lewkow, N.R., Kharchenko, V. (2014), Precipitation of Energetic Neutral Atoms and Induced Non-thermal Escape Fluxes from the Martian Atmosphere. *The Astrophysical Journal* 790, 98. 10.1088/0004-637X/790/2/98
Description: Connections between parameters of precipitating fast ions and resulting escape fluxes, altitude-dependent energy distributions of fast atoms and their coefficients of reflection from the Mars atmosphere, are established using accurate cross sections in Monte Carlo (MC) simulations. Distributions of secondary hot (SH) atoms and molecules, induced by precipitating particles, have been obtained and applied for computations of the non-thermal escape fluxes.

Li, X., Huang, Y.L., Flesch, G.D., Ng, C.Y. (1997), A state-selected study of the ion-molecule reactions $\text{O}^+(\text{}^4\text{S}, \text{}^2\text{D}, \text{}^2\text{P}) + \text{N}_2$. *Journal of Chemical Physics* 106, 1373. 10.1063/1.474087
Description: Absolute state-selected cross sections for the reactions $\text{O}^+(\text{}^4\text{S}, \text{}^2\text{D}, \text{}^2\text{P}) + \text{N}_2$ to $\text{N}_2^+ + \text{O}$, $\text{NO}^+ + \text{N}$, and $\text{N}^+ + \text{NO}$ (and/or $\text{N}^+ + \text{N} + \text{O}$) have been measured in the center-of-mass collision energy ($E_{\text{c.m.}}$) range of 0.06-40 eV employing the differential retarding potential method and the $\text{O}^+(\text{}^2\text{D})$ and $\text{O}^+(\text{}^2\text{P})$ ion state-selection schemes we developed recently.

Lindsay, B.G., Sieglaff, D.R., Smith, K.A., Stebbings, R.F. (2001), Charge transfer of keV O^+ ions with atomic oxygen. *Journal of Geophysical Research* 106, 8197. 10.1029/2000JA000437
Description: We report absolute differential cross sections for charge transfer scattering of 0.5-5 keV $\text{O}^+(\text{}^4\text{S})$ ground state and $\text{O}^+(\text{}^2\text{D}, \text{}^2\text{P})$ metastable ions by atomic oxygen at angles between 0.04 degrees and 3 degrees in the laboratory frame.

Lindsay, B.G., Merrill, R.L., Straub, H.C., Smith, K.A., Stebbings, R.F. (1998), Absolute differential and integral cross sections for charge transfer of keV O^+ with N_2 . *Physical Review A* 57, 331. 10.1103/PhysRevA.57.331

Description: We report measurements of the absolute differential cross sections for charge transfer scattering of 0.5-, 0.85-, 1.5-, 2.8-, and 5-keV O^+ by N_2 at scattering angles between 0.04 degrees and 3.1 degrees in the laboratory frame. Cross sections for both $O^+(^4S)$ ground-state and $O^+(^2D, ^2P)$ metastable projectiles are presented.

Lishawa, C. Randal, Dressler, Rainer A., Gardner, James A., Salter, Richard H. and Murad, Edmond (1990), Cross sections and product kinetic energy analysis of $H_2O^+ + H_2O$ collisions at suprathermal energies, J. Ch. Ph., 93, 3196-3206. 10.1063/1.458852
Description: The reaction of H_2O^+ with H_2O is studied using a longitudinal geometry double mass spectrometer in the collision energy range $E_{c.m} = 0.5$ -25 eV.

Lo, H. H., Kurzweg, L., Brackman, R. T., Fite, W. L. (1971), Electron Capture and Loss in Collisions of Heavy Ions with Atomic Oxygen, Physical Review A 4, 1462. 10.1103/PhysRevA.4.1462

Description: Electron-capture and electron-loss cross sections for various gaseous (N^+ , O^+ , Ar^+ , Kr^+ , and Xe^+) and metallic (Al^+ , K^+ , Fe^+ , Ba^+ , and Ba^{++}) ions in collisions with atomic oxygen have been measured in the energy range 30 keV to 2 MeV.

Luna, H., et al. (2005), Dissociative Charge Exchange and Ionization of O_2 by Fast H^+ and O^+ Ions: Energetic Ion Interactions in Europa's Oxygen Atmosphere and Neutral Torus. The Astrophysical Journal 628, 1086. 10.1086/431140

Description: Measurements of electron capture and ionization of O_2 molecules in collisions with H^+ and O^+ ions have been made over an energy range 10-100 keV. Cross sections for dissociative and nondissociative interactions have been separately determined using coincidence techniques.

Luna, H., et al. (2003), Dissociation of N_2 in capture and ionization collisions with fast H^+ and N^+ ions and modeling of positive ion formation in the Titan atmosphere, J. Geophys. Res. 108, NO.E4, 5033. 10.1029/2002JE001950

Description: Electron capture and ionization cross sections for protons and nitrogen ions incident on N_2 are measured in the energy range 10–100 keV using time of flight (TOF) coincidence counting techniques.

McClure, G.W. (1966), Electron Transfer in Proton-Hydrogen-Atom Collisions: 2-117 keV. Physical Review 148, 47. 10.1103/PhysRev.148.47

Description: The cross section for electron transfer between a proton and a hydrogen atom has been measured in the energy range 2 to 117 keV.

McGrath, M.A., Johnson, R.E. (1989), Charge exchange cross sections for the Io plasma torus. Journal of Geophysical Research 94, 2677. 10.1029/JA094iA03p02677

Description: An impact parameter method for calculating cross sections as a function of incident ion energy is used in conjunction with an improved exchange energy formulation to update several of the charge exchange cross sections currently used in Io plasma torus modeling. New cross sections for $S^+ + S_2^+ \Rightarrow S_2^+ + S^+$ and Na^+ on neutral targets, useful in analyzing the fast Na jets observed at Io, are also calculated.

Moran, T.F., Wilcox, J.B. (1978), Charge transfer reactions of ground $O^+(^4S)$ and excited $O^+(^2D)$ state ions with neutral molecules. *Journal of Chemical Physics* 69, 1397. 10.1063/1.436752

Description: Total charge transfer cross sections have been measured for the reactions of 0.6 to 3.0 keV $O^+(^4S)$ and $O^+(^2D)$ ions with Ar, H₂, N₂, O₂, CO, NO, and CO₂. Time-of-flight techniques have been used to measure the fast neutral O products from charge transfer reactions in which reactant O^+ ion beams have been produced by controlled electron impact ionization of oxygen.

Newman, J.H., et al. (1982), Charge transfer in $H^+ + H$ and $H^+ + D$ collisions within the energy range 0.1-150 eV. *Physical Review A* 25, 2976. 10.1103/PhysRevA.25.2976

Description: Absolute charge-transfer cross sections for collisions of protons with hydrogen and deuterium atoms have been measured within the energy range 0.1 to 150 eV using the merging-beams technique. The results are in excellent agreement with a fully quantum-mechanical treatment of this reaction.

Nutt, W.L., McCullough, R.W., Gilbody, H.B. (1979), Electron capture by 0.1-13 keV C^+ , N^+ and O^+ ions in H and H₂. *Journal of Physics B Atomic Molecular Physics* 12, L157. 10.1088/0022-3700/12/5/005

Description: Cross sections for one-electron capture by C^+ , N^+ and O^+ ions in H and H₂ have been investigated within the energy range 0.1-13 keV from measurements using a tungsten tube furnace to provide a target of highly dissociated hydrogen.

Orient, O.J., and S.K. Srivastava (1987), Electron impact ionization of H₂O, CO, CO₂ and CH₄. *J. Phys. B Atomic Molecular Physics* 20, 2923-3936. 10.1088/0022-3700/20/15/036

Description: Utilising a crossed electron-beam-molecular-beam collision geometry and the relative flow technique normalised values of total and partial ionisation cross sections for H₂O, CO, CO₂ and CH₄ have been measured.

Phaneuf, R. A. et al. (1987), Atomic data for fusion, Published and Edited by Controlled Fusion Atomic Data Center H. T. Hunter.

Description: Available cross-section data for heavy-particle collision processes which play important roles in the edge plasma of magnetically-confined fusion devices are surveyed and reviewed. The species considered include H, H₂, He, C, O, Fe, and their ions.

Phaneuf, R. A. et al. (1978), Single-electron capture by multiply charge ions of carbon, nitrogen, and oxygen in atomic and molecular hydrogen, *Phys. Rev.* 17534-545. 10.1103/PhysRevA.17.534

Description: Cross sections for electron capture by N^+ , C^+ , and O^+ incident on atomic and molecular hydrogen have been measured in the velocity range $(0.3-5.2) \times 10^8$ cm/s.

Phelps, A. V. (1991), Cross Sections and Swarm Coefficients for Nitrogen Ions and Neutrals in N₂ and Argon Ions and Neutrals in Ar for Energies from 0.1 eV to 10 eV, *J. Phys. Chem. Ref. Data* 20, 557-573. 10.1063/1.555889

Description: Graphical and tabulated data and the associated bibliography are presented for cross sections for elastic, excitation, and ionization collisions of N^+ , N_2^+ , N , and N_2 with N_2 and for Ar^+ and Ar with Ar for laboratory energies from 0.1 eV to 10 keV.

Pivovarov, L.I., Nikolaichuk, L.I., Grigor'ev, A.N. (1969), Charge Exchange of Alkali Metal Ions in Alkali Metal Vapor and Inert Gases. Soviet Journal of Experimental and Theoretical Physics 30, 236.

Description: No abstract.

Rao, M. V. V. S., Iga, and S. K. Srivastava (1995), Ionization cross-sections for the production of positive ions from H_2O by electron impact, J. Geophys. Res., 100(E12), 26421-26425. 10.1029/95JE02314

Description: Cross-section values for the direct and dissociative ionization of H_2O by electron impact have been measured and compared with previously published data. The present measurements have been carried out from thresholds to 1 keV by utilizing a crossed electron beam and molecular beam collision geometry and an improved ion extraction technique.

Rees, M.H. (1989), Physics and Chemistry of the Upper Atmosphere. Physics and Chemistry of the Upper Atmosphere.

Description: A multitude of processes that operate in the upper atmosphere are revealed by detailed physical and mathematical descriptions of the interactions of particles and radiation, temperatures, spectroscopy and dynamics.

Rudd, M.E., Kim, Y.K., Madison, D.H., Gallagher, J.W. (1985), Electron production in proton collisions: total cross sections. Reviews of Modern Physics 57, 965. 10.1103/PhysRevA.28.3244

Description: Using the parallel-plate-capacitor method and a capacitance manometer to determine pressures, total cross sections for the production of positive and negative charges were measured for 5-4000 keV proton impact on He, Ne, Ar, Kr, H_2 , N_2 , CO, O_2 , CH_4 , and CO_2 . From these, ionization and electron-capture cross sections were obtained and fitted to semiempirical equations describing the energy dependence in terms of a few parameters.

Rudd, M.E., Goffe, T.V., Dubois, R.D., Toburen, L.H., Ratcliffe, C.A. (1983), Cross sections for ionization of gases by 5-4000 keV protons and for electron capture by 5-150 keV protons. Physical Review A 28, 3244. 10.1103/RevModPhys.57.965

Description: Existing data on the ionization of neutral atoms and molecules by proton impact are reviewed, and electron production cross-section data are collected. The three major experimental methods are discussed and possible sources of error identified.

Shah, M.B., Latimer, C.J., Montenegro, E.C., et al. (2009), The Implantation and Interactions of O^+ in Titan's Atmosphere: Laboratory Measurements of Collision-induced Dissociation of N_2 and Modeling of Positive Ion Formation, Ap.J., 703, 1947. 10.1088/0004-637X/703/2/1947

Description: Energetic oxygen ions are an important component of the plasma incident onto Titan's atmosphere. Therefore, we report measurements of electron capture and ionization collisions of N₂ with incident O⁺ over the energy range 10-100 keV. Using time of flight coincidence counting techniques we also measured the collision-induced dissociation of N₂ following ionization and electron capture.

Shah, M.B., Geddes, J., McLaughlin, B.M., Gilbody, H.B. (1998), LETTER TO THE EDITOR: New low-energy measurements and calculation of ionization in H⁺ + H collisions. Journal of Physics B Atomic Molecular Physics 31, L757. 10.1088/0953-4075/31/19/001

Description: In response to the strong current theoretical interest in models of low-energy ionization collisions, a crossed-beam coincidence counting technique previously used in this laboratory to obtain cross sections has been successfully adapted to extend the measurements downwards in energy.

Shah, M.B., McCallion, P., Gilbody, H.B. (1989), Ionisation and electron capture in collisions of slow H⁺ and He²⁺ ions with hydrogen. Journal of Physics B Atomic Molecular Physics 22, 3983. 10.1088/0953-4075/22/24/006

Description: A crossed-beam technique previously used in the authors' laboratory for studies of ionisation of H₂ by H⁺ and He²⁺ impact in the ranges 38-1500 and 31-550 keV amu⁻¹, respectively, has been adapted to permit measurements to be extended down to 10 keV amu⁻¹. Both ionisation and electron capture have been studied using time-of-flight mass spectroscopy together with electron-slow-ion and slow-ion-fast-ion coincidence counting of the collision products.

Shah, M.B., Elliott, D.S., Gilbody, H.B. (1987), Ionisation of atomic hydrogen by 9-75 keV protons. Journal of Physics B Atomic Molecular Physics 20, 2481. 10.1088/0022-3700/20/11/016

Description: A crossed beam method incorporating time-of-flight analysis and coincidence counting of the collision products was used previously in this laboratory to study H⁺ + H ionisation in the range 38-1500 keV. The same approach has now been used to extend measurements down to 9.4 keV.

Sieglaff, D.R., Lindsay, B.G., Smith, K.A., Stebbings, R.F. (1999), Absolute differential and total cross sections for charge transfer of O⁺ with H₂. Physical Review A 59, 3538. 10.1103/PhysRevA.59.3538

Description: Absolute differential cross sections (DCS's) are reported for charge-transfer scattering of 0.5-, 0.85-, 1.5-, 2.8-, and 5.0-keV O⁺ ions by H₂ molecules at angles between 0.04 degrees and 5.4 degrees in the laboratory frame. Cross sections for O⁺(⁴S) ground state and O⁺(²D,²P) metastable ions are presented.

Stebbing, R. F. et al. (1963a), Charge Transfer in Oxygen, Nitrogen, and Nitric Oxide, J. Chem. Phys. 38, 2277-2279. 10.1063/1.1733961

Description: The cross sections for charge transfer in collisions of N₂ and O₂ with various atomic and molecular ions have been measured within the energy range 30 to 10,000 eV.

Modulated-crossed-beam techniques were used and the relative cross sections so obtained were normalized with the aid of absolute measurements made by Stier and Barnett.

Stebbing, R. F. et al. (1963b), Charge Transfer between Some Atmospheric Ions and Atomic Oxygen, *J. Chem. Phys.* 38, 2280-2284. 10.1063/1.1733962

Description: Cross sections for charge transfer between oxygen atoms and N^+ , N_2^+ , NO^+ , and O_2^+ ions have been measured within the energy range 50 to 10,000 eV, using modulated-crossed-beam techniques.

Stier, P.M., Barnett, C.F. (1956), Charge Exchange Cross Sections of Hydrogen Ions in Gases. *Physical Review* 103, 896. 10.1103/PhysRev.103.896

Description: Measurements are reported of the cross section for electron capture, electron loss, and electron detachment for hydrogen atoms and ions traversing several gases.

Straub, H. C.; Lindsay, B. G.; Smith, K. A.; Stebbings, R. F. (1998), Absolute partial cross sections for electron-impact ionization of H_2O and D_2O from threshold to 1000 eV, *J. Ch. Ph.*, 108, 109-116. 10.1063/1.475367

Description: Absolute partial cross sections for electron-impact ionization of H_2O and D_2O are reported for electron energies from threshold to 1000 eV.

H. Tawara, T. Kato, Y. Nakai (1985), Cross sections for electron capture and loss by positive ions in collisions with atomic and molecular hydrogen, *Atomic Data and Nuclear Data Tables*, Volume 32, Issue 2, 235-303. 10.1016/0092-640X(85)90007-5

Description: Experimental cross sections for electron capture and loss by atomic positive ions in collisions with atomic and molecular hydrogen targets are tabulated as a function of the incident energy of projectile ions and of their charge state.

Thompson, W.R., Shah, M.B., Geddes, J., Gilbody, H.B. (1997), LETTER TO THE EDITOR: Ionization of atomic oxygen by protons. *Journal of Physics B Atomic Molecular Physics* 30, L207. 10.1088/0953-4075/30/6/004

Description: A crossed-beam technique incorporating time-of-flight analysis and coincidence counting of the collision products, recently used in this laboratory to study one-electron capture in collisions of H^+ ions with ground-state oxygen atoms, has been adapted to allow measurements of the corresponding cross sections for ionization for the first time.

Thompson, W.R., Shah, M.B., Gilbody, H.B. (1996), One-electron capture in collisions of 6-100 keV protons with oxygen atoms. *Journal of Physics B Atomic Molecular Physics* 29, 725. 10.1088/0953-4075/29/4/014

Description: A crossed-beam technique incorporating time-of-flight analysis and coincidence counting of the collision products has been used to study one-electron capture by 6-100 keV protons in collisions with oxygen atoms.

Tully, C., Johnson, R.E. (2002), Semiclassical calculation of collisional dissociation cross sections for $N+N_2$. *Journal of Chemical Physics* 117, 6556. 10.1063/1.1504085

Description: Dissociation and doubly differential cross sections are calculated for $N+N_2$ at near-threshold collision energies using a semiclassical wave packet method in which the vibrational motion of the molecule is treated quantum mechanically and the rotational and translational motions are treated classically. A three-bodied London-Eyring-Polanyi-Sato potential energy surface is used and results compared to those obtained using a purely repulsive power law potential.

Tully, C., Johnson, R.E. (2001), Low energy collisions between ground-state oxygen atoms. *Planetary and Space Science* 49, 533. 10.1016/S0032-0633(01)00002-2

Description: Elastic scattering cross sections have been calculated for the $O(^3P)+O(^3P)$ collision at energies $E=1-10$ eV using exact quantum calculations and the semiclassical Jeffries-Wentzel-Kramers-Brillouin approximation with the full set of 18 states of O_2 which separate to this system.

Xu, Y., Thomas, E.W., Moran, T.F. (1990), Charge transfer reactions of ground $O^+(^4S)$ and metastable $O^+(^2D, ^2P)$ ions with H_2 molecules. *Journal of Physics B Atomic Molecular Physics* 23, 1235. 10.1088/0953-4075/23/7/019

Description: Cross sections for charge transfer reactions of ground $O^+(^4S)$ and metastable $O^+(^2D, ^2P)$ state ions with H_2 have been measured for reactant ions with 10 to 500 eV kinetic energies.